Responsiveness of Retinal Ganglion Cells Through Frequency Modulation of Electrical Stimulation: A Computational Modeling Study

Javad Paknahad *Student Member, IEEE*, Kyle Loizos *Member, IEEE*, Mark Humayun, *Fellow*, IEEE, and Gianluca Lazzi, *Fellow, IEEE*

Abstract— Electrical stimulation of surviving retinal neurons has proven effective in restoring sight to totally blind patients affected by retinal degenerative diseases. Morphological and biophysical differences among retinal ganglion cells (RGCs) are important factors affecting their response to epiretinal electrical stimulation. Although detailed models of ON and OFF RGCs have already been investigated, here we developed morphologically and biophysically realistic computational models of two classified RGCs, D1-bistratified and A2monostratified, and analyzed their response to alternations in stimulation frequency (up to 200 Hz). Results show that the D1bistratified cell is more responsive to high frequency stimulation compared to the A2-monostratified cell. This differential RGCs response suggests a potential avenue for selective activation, and in turn different encoded percept of RGCs.

I. INTRODUCTION

RETINAL implants have been developed to restore partial sight to patients who have been blinded for decades by degenerative diseases, such as retinitis pigmentosa (RP) and age-related macular degeneration (AMD). These devices stimulate surviving neurons in the degenerated retina to elicit visual percepts. This approach has proven effective and led to the development of several retinal prosthetic devices [1].

A main challenge with current epiretinal prosthetic systems is the inability to focally activate a population of RGCs. Reports from clinical studies have revealed that axonal activation of RGCs can result in elongated phosphenes [2]. Many studies have focused on designing electrical stimulation strategies to improve efficacy and spatial resolution of currently implanted devices [3], [4]. Further understanding of how different subtypes of RGCs respond to electrical stimulation, and the mechanism underlying the preferential activation of each cell type, could significantly improve the efficacy of retinal prostheses.

Although research has been conducted considering ON and OFF RGC subtypes and their responses to electrical stimulation [5], there are only few computational modeling studies of both biophysically and morphologically classified

RGCs, in particular bistratified RGC subtypes. Furthermore, there have been studies for preferentially targeting ON and OFF RGCs at high stimulation frequency (> 2 kHz) [6], [7], but no particular work on stimulus waveforms designs for excitation of select RGC subtypes. These classified RGCs carry specific types of visual information, such as color and contrast, features which may be possible to induce with selective stimulation. For example, the findings in studies that have shown the contribution of small bistratified ganglion cells to "blue-yellow" color opponency in the retinal circuitry could be leveraged [8].

Recently, biophysical properties of different ganglion cell types using single-compartmental models have been estimated based on the experimental data taken in-vitro from rat retina [9]. In this paper, we develop biophysically and morphologically detailed models of the D1-bistratified and the A2-monostratified RGCs and validate their responses with experimentally recorded signals reported in [9]. We further apply a AM-NEURON multi-scale computational platform developed by our group [10]-[14] to determine whether different retinal cells exhibit different responses (e.g. firing rate) as a function of parameters such as the stimulation frequency (up to 200 Hz). The differential frequency response of RGCs can potentially help establishing the mechanism to preferentially activate subtypes of RGCs.

II. METHODS

In this study, we utilized our three-dimensional Admittance Method/NEURON multi-scale computational modeling platform to predict the electric fields generated inside retinal tissue, coupled to multi-compartmental models of neurons in order to determine the activation of realistic RGCs. Admittance method linked with NEURON has proven a powerful approach not only for studies of field distribution inside the tissue due to electrical stimulation, but also providing a platform to analyze realistic representations of various cell types [10]-[15].

*This work was supported by the NSF EAGER (Award No. 1833288), the NEI (NIH Grant No. R21EY028744), the NIBIB (NIH Grant No. U01EB025830), and an unrestricted grant to the Department of Ophthalmology from Research to Prevent Blindness, New York, NY.

J. Paknahad, and K. Loizos are with the Department of Electrical Engineering University of Southern California, Los Angeles, CA 90089 USA (paknahad@usc.edu).

M. Humayun is with the Departments of Ophthalmology and Biomedical Engineering, University of Southern California, Los Angeles, CA 90033 USA.

G. Lazzi is with the Departments of Ophthalmology and Electrical Engineering, University of Southern California, Los Angeles, CA 90089 USA

A. Admittance Method: Constructing the Retina Tissue and Electrodes

In this approach, a computational model of the retina tissue and implant electronics are discretized, and electrical properties are assigned to each voxel in the model. A current source is applied as an input and the resulting voltage is computed at each node in the voxel. Then, a linear interpolation function is used to obtain the voltage at the center of each neuronal compartment, which is utilized for the computation of the neural response using NEURON [16]. Further details can be found in [10]-[13]. Although the AM-NEURON computational platform is now parallelized and accommodates adaptive multiresolution meshing, for the specific case considered here we have adopted a uniform model resolution set to 10 µm.

To represent the degenerated retina tissue, the thickness of the outer part of the retina which consists of outer plexiform and outer nuclear layers were mostly reduced. The retina laminar properties are identical to those utilized in our previous work [10]. The computational model of a stimulating electrode of diameter 200 µm is placed on the center of the bulk retina tissue, which is discretized in 2 million computational cells, and is positioned 50 µm from the cell bodies of computational models of the RGCs. The resistivity of platinum (10.6 \times 10⁻⁸ Ω .m) is utilized in the model of the electrode, which is surrounded by insulating material. The admittance method was then used to solve the voltage generated inside the tissue by the stimulus current. For studying the RGC's frequency response, we used a symmetric charge-balanced biphasic pulse of constant pulse width (0.5 ms) and amplitude (100 µA), with no interphase gap (IPG). Stimulus frequency ranging from 6 Hz to 200 Hz (6, 20, 40, 60, 120, and 200 Hz) were considered. Resulting extracellular voltages were applied to multi-compartment models of neurons and computation executed using embedded NEURON software. Neuronal responses of individual retinal ganglion cells were then recorded.

B. NEURON Model

The morphology of ganglion cell types was extracted as SWC files from the NeuroMorpho dataset [17], [18] and imported to NEURON software. The extracted cells are of types A2 and D1, and their morphological parameters can be found in [19]. Fig. 1 shows the morphology of these two cells, including the levels of stratification in the inner plexiform layer of the retina. As shown, D1-bistratified cells consist of two levels of dendritification, in which one layer of the dendritic tree is ramified inside the inner part, and another is placed in the outer section of the inner plexiform layer. The dendritic structure of the A2-monostratified cell types is only distributed in the inner part of the inner plexiform layer.

These morphologically realistic cells are compartmentalized and their responses to electrical stimulation are solved based on multi-compartment Hodgkin–Huxley models. Each compartment includes several ionic channels, and they are modeled as voltage-dependent conductances in parallel with the membrane capacitance. In addition to the five ionic channel models from *Fohlmeister and Miller* [20], [21] for the

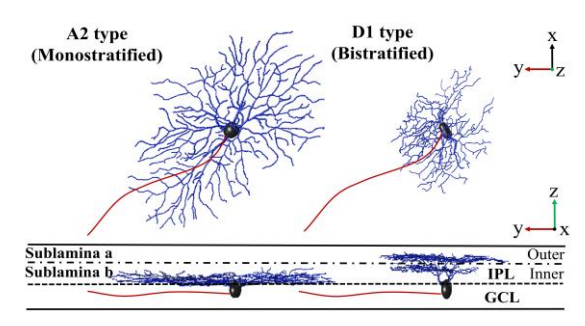


Fig. 1. A2 and D1 realistic morphologies as implemented and coded in our multiscale Admittance Method/NEURON computational platform. *Left:* A2-monostratified RGC ramified in the inner part of inner plexiform layer and has a larger soma and dendritic field diameters. *Right:* D1-bistratified, their dendrites are placed in both inner and outer part of the inner plexiform layer and this cell has relatively smaller soma and dendritic field dimeters.

ganglion cells, two more ionic currents have been considered to more accurately represent the intrinsic electrophysiological properties of different ganglion cell types including the difference between ON and OFF cell types and the phenomenon such as rebound excitation, which plays a fundamental role in encoding visual percepts [22]. The hyperpolarization-activated, LVA calcium ionic channels were modelled as in [23], and [24] respectively. The reversal potentials of these channels, the time-dependent reversal potential equation of calcium channel, E_{Ca} , and the ligand gated, $g_{\text{k,Ca}}$, formula are similar to those in [9], [20]. The gating variables m, h, c, n, a, h_A, l, m_T were described using first-order kinetic equation:

$$\frac{dx}{dt} = -(\alpha_x + \beta_x)x + \alpha_x \tag{1}$$

where α and β are rate constants for voltage-dependent ion channels, and x is the gating variable. However, the gating variable for the hyperpolarization-activated current (h_T) does not follow the above formula. The rate of transition for I_T current is the second-order dynamic as following:

$$egin{align} rac{dh_T}{dt} &= lpha_{h_T}(1-h_T-d) - eta_{h_T}h_T \ &rac{dd}{dt} &= eta_d(1-h_T-d) - lpha_dd \ \end{aligned}$$

The expressions of rate constants for different ionic channels are given in Table I.

Recently, a single-compartment model of ganglion cell was used to find the constraints for the maximum ionic conductance values, in which the model output can replicate the electrophysiological properties of different RGC types [9]. We first reproduced the results of this paper and then further developed the RGC models to include multicompartment representations and tuned the density of ion channels accordingly in soma, dendrites and axon. In addition, since the axons were missing from the available morphologies, the axonal morphology (1 µm in diameter) was extracted from another dataset and added to both cell types considered in this study.

Due to the lack of voltage-clamp data on axons of different RGCs, biophysics are assumed to be identical for both D1 and A2 cells. The experimentally recorded signals of A2 and D1 cells were used for the model tuning. The range of variation in the density of ion channels of the dendrites, and axon is based upon the constraints demonstrated by *Fohlmeister et al.* [25]. The tuned biophysical properties of both A2 and D1 cells for the soma, dendrites, and axon are provided in Table II

C. Extracellular stimulation: Admittance method linked with NEURON

For the extracellular stimulation of the retina tissue, the admittance method was used to calculate the resulting voltage at each node for a given input current. The voltage at the center of each voxel was estimated using a linear interpolation function. Since the Admittance method and NEURON have the same coordinates, a computational code was developed to superimpose the potential computed in the tissue volume into the NEURON model and apply it as an extracellular voltage, using "extracellular" mechanism built in NEURON software, to each compartment in the Hodgkin–Huxley circuit in series with the membrane [10].

The modeled RGCs were validated by comparing results with the experimentally recorded signals provided in [9]. Individual responses of both A2 and D1 ganglion cell types to extracellular epiretinal stimulation were computed using a range of stimulus frequency with the goal of identifying the responsiveness of D1-RGCs compared to A2-RGC at high frequency of stimulation.

III. RESULTS

A. Intracellular Stimulation

Fig. 2 shows that the morphologically and biophysically realistic models of RGCs that closely reproduce the measured

TABLE I
RATE CONSTANTS OF IONIC CURRENTS

Na Channel	$\begin{split} \alpha_m &= \frac{-0.6 (E+30)}{e^{-0.1 (E+30)} - 1} \\ \alpha_h &= 0.4 \; e^{-(E+50)/20} \end{split}$	$\beta_m = 20 \ e^{-(E+55)/18}$ $\beta_h = \frac{6}{e^{-0.1(E+20)} + 1}$
Ca Channel	$\alpha_c = \frac{-0.3(E+13)}{e^{-0.1(E+13)}-1}$	$\beta_c = 10 \ e^{-(E+38)/18}$
K Channel	$\alpha_n = \frac{-0.02 (E+40)}{e^{-0.1 (E+40)}-1}$	$\beta_n = 0.4 \ e^{-(E+50)/80}$
A Channel	$\begin{split} \alpha_A &= \frac{-0.006 (E+90)}{e^{-0.1 (E+90)} - 1} \\ \alpha_{h_A} &= 0.04 \; e^{-(E+70)/20} \end{split}$	$\beta_A = 0.1 \ e^{-(E+30)/10}$ $\beta_{h_A} = \frac{0.6}{e^{-0.1(E+40)} + 1}$
h Channel	$\alpha_l = e^{0.08316(E + 75)}$	$\beta_l = e^{0.033264(E+75)}$
T Channel	$\begin{split} &\alpha_{m_T} = \left(1.7 + e^{-(E + 28.8)/13.5}\right)^{-1} \\ &\alpha_{h_T} = e^{-(E + 160.3)/17.8} \\ &\alpha_{d} = \frac{1 + e^{(E + 37.4)/30}}{240\left(0.5 + \left(0.25 + e^{(E + 83.5)/6.3}\right)^{0.5}\right)} \end{split}$	$\begin{split} \beta_{m_T} &= \frac{e^{-(E+63)/7.8}}{1.7 + e^{-(E+28.8)/13.5}} \\ \beta_{h_T} &= \alpha_{h_T} ((0.25 + e^{(E+83.5)/6.3})^{0.5} - 0.5 \\ \beta_d &= \alpha_d \big(0.25 + e^{(E+83.5)/6.3}\big)^{0.5} \end{split}$

TABLE II MAXIMUM IONIC CONDUCTANCE VALUES FOR A2 AND D1 CELLS $[S/cm^2]$.

	RGC types						
	A2			D1			
	Soma	Dendrite	Axon	Soma	Dendrite	Axon	
g _{Na}	0.3	0.1	0.8	0.2	0.08	0.8	
g_K	0.12	0.05	0.6	0.211	0.08	0.6	
$g_{K,A}$	3*g _K	$3*g_K$	$3*g_K$	$3*g_K$	$3*g_K$	$3*g_K$	
$g_{K,\mathrm{Ca}}$	0.004*g _K	0.004*g _K	-	0.004* g _K	$0.004*g_{K}$	-	
g_{Ca}	0.037	0.05	-	0.013	0.01	-	
g_h	0	0	-	0.0001	3e-5	-	
g_{T}	0.004	0	-	0.002	0.001	-	

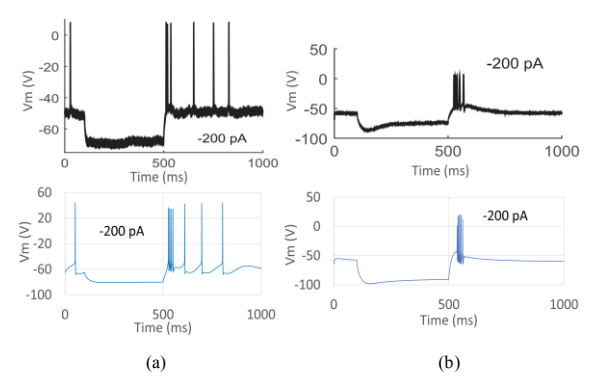


Fig. 2. Comparison between experimental (top) and computational (bottom) membrane voltages in the cell body (soma) in response to intracellular stimulation. The hyperpolarizing step current stimulation was applied between 100 ms and 500 ms. (a): A2 cell; (b): D1 cell. Experimental data obtained from [9].

electrophysiological responses provided in [9]. For this validation, intracellular hyperpolarizing step currents of 200 pA with 400 ms duration were injected to the cells and their responses were recorded from the cell body soma running NEURON simulations. As illustrated, the RGC's model can closely replicate the behavior of the experimentally recorded cells, including the rebound excitation phenomenon, which is described as action potentials initiation after termination of a hyperpolarizing current. The intrinsic physiological properties of the modeled RGCs meet the constraints on the experimental data provided in [9].

B. Extracellular Stimulation: Frequency Response

We applied symmetric charged-balance electrical stimulation waveforms to characterize RGCs cellular selectivity as a function of stimulation frequency. We compared the responses of D1-bistratified versus A2-monostratified RGCs to alternations in stimulation frequency. Fig. 3 shows the firing rates of both A2 and D1 cells as a function of the stimulation frequency.

As shown in the figure, the firing rate of the D1 cell is higher compare to the A2 cells at higher frequencies. The results demonstrate that the spiking rate observed in the A2-monostratified cell cannot follow the stimulus pulses with a similar rate. However, each stimulus pulse that applied to the D1-cell results in firing of action potentials. The importance of this finding lies in the potential to exploit this differential

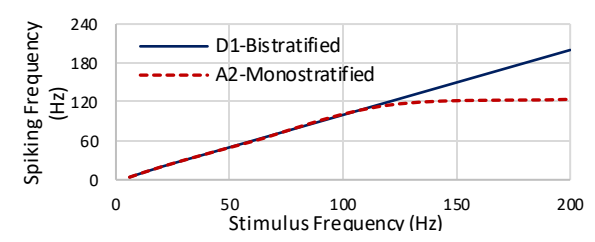


Fig. 3. Preliminary computational results showing the difference in frequency response between A2 and D1 retinal ganglion cells. The difference in the computationally determined frequency response can potentially help identifying the mechanism to selectively target RGCs.

RGC response in retinal prosthetic systems by varying stimulation frequency to induce a different percept.

IV. DISCUSSION

A multi-scale computational study using a combined Admittance method-NEURON models was conducted to further our understanding of cellular selectivity of RGCs in the electrically stimulated degenerated retina. We first developed models of the two classified ganglion cells known as D1-bistratified and A2-monostratified. Their responses to electrical stimulation with alternations in stimulation frequency were further evaluated: computational results demonstrate that bistratified RGCs can evoke spikes with similar rate of stimulus pulses, while monostratified RGCs cannot manage to follow higher stimulation frequency.

In this work, we centered our focus on the difference in the size of the cell body, the dendritic structure, and the level dendritification of the two classified RGCs assuming similar axonal properties. In the future, we will perform statistical and sensitivity analysis considering the effects of morphological factors such as the diemeter of RGCs axon on the firing rates.

This study is motivated by our intent to identify mechanisms that will allow us to potentially encode additional information in a visual prosthetic system if a response in the same location of the stimulation of the retina can be modulated by using different frequencies of stimulation. For example, prevailing research indicates that stimulation frequency may play a role in the percept of color [26]: the methods presented in this paper may aid in the understanding of this differential percept and ultimately provide insights toward the development of visual prosthetic systems with increased information content for the patient. Future work will focus on the correlation of experiential percept by patient with predicted firing rates of different class of RGCs, with the goal of elucidating the mechanisms primarily responsible for different color percept by patient.

REFERENCES

- [1] D. Weiland, "Retinal Prosthesis," *Annual Review of Biomedical Engineering*, vol. 61, no. 5, pp. 24–1412, 2014.
- [2] M. Beyeler *et al*, "A model of ganglion axon pathways accounts for percepts elicited by retinal implants," *BioRxiv*, pp. n/a, 2018.
- [3] A. E. Hadjinicolaou et al, "Optimizing the electrical stimulation of retinal ganglion cells," *IEEE Transactions on Neural Systems and Rehabilitation Engineering*, vol. 23, no. 2, pp. 169-178, 2015.

- [4] Y. Chang et al, "Stimulation strategies for selective activation of retinal ganglion cell soma and threshold reduction," *Journal of Neural Engineering*, vol. 16, no. 2, pp. 026017, 2019.
- [5] T. Guo et al, "Cell-specific modeling of retinal ganglion cell electrical activity," Conference Proceedings: Annual International Conference of the IEEE Engineering in Medicine and Biology Society. IEEE Engineering in Medicine and Biology Society. Annual Conference, vol. 2013, pp. 6539-6542, 2013.
- [6] T. Guo et al, "Selective activation of ON and OFF retinal ganglion cells to high-frequency electrical stimulation: A computational modeling study," The Institute of Electrical and Electronics Engineers, Inc. (IEEE) Conference Proceedings, pp. 6108-6111, 2014.
- [7] T. Guo et al, "Mediating Retinal Ganglion Cell Spike Rates Using High-Frequency Electrical Stimulation," Frontiers in Neuroscience, 2019.
- [8] D. M. Dacey, J. D. Crook and O. S. Packer, "Distinct synaptic mechanisms create parallel S-ON and S-OFF color opponent pathways in the primate retina," Vis. Neurosci., vol. 31, no. 2, pp. 139-51, 2014.
- [9] W. Qin et al, "Single-compartment models of retinal ganglion cells with different electrophysiologies," *Network*, vol. 28, no. 2-4, pp. 74-93, 2017
- [10] K. Loizos et al, "Increasing electrical etimulation efficacy in degenerated retina: stimulus waveform design in a multiscale computational model," *IEEE Transactions on Neural Systems and Rehabilitation Engineering*, vol. 26, no. 6, pp. 1111-1120, 2018.
- [11] K. Loizos et al, "A multi-scale computational model for the study of retinal prosthetic stimulation," The Institute of Electrical and Electronics Engineers, Inc. (IEEE) Conference Proceedings, pp. 6100-6103, 2014.
- [12] C. J. Cela, R. C. Lee and G. Lazzi, "Modeling cellular lysis in skeletal muscle due to electric shock," *IEEE Trans. Biomed. Eng.*, vol. 58, no. 5, pp. 1286-1293, 2011.
- [13] C. J. Cela, "A multiresolution admittance method for large-scale bioelectromagnetic interactions." Ph.D., North Carolina State University, United States -- North Carolina, 2010.
- [14] C. S. Bingham et al, "Model-based analysis of electrode placement and pulse amplitude for hippocampal stimulation," *IEEE Trans. Biomed. Eng.*, vol. 65, no. 10, pp. 2278-2289, 2018.
- [15] J. Stang et al, "Recent Advances in Computational and Experimental Bioelectromagnetics for Neuroprosthetics," The Institute of Electrical and Electronics Engineers, Inc. (IEEE) Conference Proceedings, pp. 1382, 2019.
- [16] M. L. Hines and N. T. Carnevale, "The neuron simulation environment," Neural Computation, vol. 9, pp. 1179-209, 1997.
- [17] NeuroMorpho.Org.
- [18] G. A. Ascoli, "Mobilizing the base of neuroscience data: the case of neuronal morphologies," *Nature Reviews Neuroscience*, vol. 7, no. 4, pp. 318-24, 2006.
- [19] C. Yin-Peng and Chuan-Chin Chiao, "Spatial distribution of excitatory synapses on the dendrites of ganglion cells in the mouse retina," *PLoS One*, vol. 9, no. 1, pp. e86159, 2014.
- [20] J. F. Fohlmeister and R. F. Miller, "Impulse encoding mechanisms of ganglion cells in the tiger salamander retina," *J. Neurophysiol.*, vol. 78, no. 4, pp. 1935-1947, 1997.
- [21] J. F. Fohlmeister, E. D. Cohen and E. A. Newman, "Mechanisms and distribution of ion channels in retinal ganglion cells: Using temperature as an independent variable," *J. Neurophysiol.*, vol. 103, no. 3, pp. 1357-1374, 2010.
- [22] T. Kameneva, H. Meffin and A. N. Burkitt, "Modelling intrinsic electrophysiological properties of ON and OFF retinal ganglion cells," *J. Comput. Neurosci.*, vol. 31, no. 3, pp. 547-561, 2011.
- [23] I. van Welie et al, "Different levels of Ih determine distinct temporal integration in bursting and regular-spiking neurons in rat subiculum," J. Physiol. (Lond.), vol. 576, pp. 203-214, 2006.
- [24] X. J. Wang, J. Rinzel and M. A. Rogawski, "A model of the T-type calcium current and the low-threshold spike in thalamic neurons," J. Neurophysiol., vol. 66, no. 3, pp. 839-850, 1991.
- [25] J. F. Fohlmeister and R. F. Miller, "Mechanisms by which cell geometry controls repetitive impulse firing in retinal ganglion cells," J. Neurophysiol., vol. 78, no. 4, pp. 1948-1964, 1997.
- [26] P. E. Stanga et al, "Patients blinded by outer retinal dystrophies are able to perceive color using the Argus II retinal prosthesis system," *Invest. Ophthalmol. Vis. Sci.*, vol. 52, no. 14, pp. 4949, 2011.